

Effect of chemical reaction, radiation and radiation absorption on the unsteady convective heat and mass transfer flow of a viscous fluid in a vertical wavy channel with oscillatory flux and heat sources

Ch. Neeraja¹, Ch. H. K. Gopal², D. R. V. Prasada Rao³ and K. Sreeranga Vani⁴

¹*Department of Mathematics, S.B.I.T Engineering College, Khammam, Telangana (India)*

²*Department of Mathematics, R.V.R & J.C Engineering College, Guntur, A.P (India)*

³*Department of Mathematics, S K University Anantapuram, AP (India)*

⁴*Department of Mathematics, Sri Satyasai Institute of Higher Learning, Anantapuram, A.P (India)*

ABSTRACT

We analyze the effect of chemical reaction, radiation, and radiation absorption on the transient convective heat and mass transfer flow of a viscous, electrically conducting fluid in a vertical wavy channel with oscillatory flux. The equations governing the flow, heat and mass transfer are solved by a regular perturbation technique with the slope δ as a perturbation parameter. The velocity, temperature, concentration, the rate of heat and mass transfer are analyzed for different variations of the governing parameters α , Q_1 , N_1 , β and K .

Keywords: Heat and Mass transfer, Chemical reaction, Radiation, Radiation absorption.

INTRODUCTION

Coupled heat and mass transfer phenomenon in porous media is gaining attention due to its interesting applications. The flow phenomenon is relatively complex rather than that of the pure thermal convection process. Underground spreading chemical wastes and other pollutants, grain storage, evaporation cooling and solidification are the few other application areas where the combined thermo-solutal natural convection in porous media are observed. Combined heat and mass transfer by free convection under boundary layer approximations has been studied by Bejan and Khair [2], Lai and Kulacki [15] and Murthy and Singh [20]. Coupled heat and mass transfer by mixed convection in Darcian fluid-saturated porous media has been analysed by Lai [14]. The free convection heat and mass transfer in a porous enclosure has been studied recently by Angirasa et al [1]. The combined effects of thermal and mass diffusion in channel flows has been studied in recent times by a few authors, notably Nelson and Wood [23,24], Lee et al [16] and others [35,38].

In recent years, energy and material saving considerations have prompted an expansion of the efforts at producing efficient heat exchanger equipment through augmentation of heat transfer. It has been established [8] that channels with diverging – converging geometries augment the transportation of heat transfer and momentum. As the fluid flows through a tortuous path viz., the dilated – constricted geometry, there will be more intimate contact between them. The flow takes place both axially (primary) and transversely (secondary) with the secondary velocity being towards the axis in the fluid bulk rather than confining within a thin layer as in straight channels. Hence it is advantageous to go for converging – diverging geometries for improving the design of heat transfer equipment. Vajravelu and Nayfeh [36] have investigated the influence of the wall waviness on friction and pressure drop of the generated coquette flow. Vajravelu and Sastry [37] have analysed the free convection heat transfer in a viscous, incompressible fluid confined between long vertical wavy walls in the presence of constant heat source. Later Vajravelu and Debnath [38] have extended this study to convective flow in a vertical wavy channel in four different geometrical configurations. This problem has been extended to the case of wavy walls by McMichael and Deutsch [19], Deshikachar et al [7], Rao et al [27] and Sree Ramachandra Murthy [31]. Hyan Goo Kwon et al [11] have

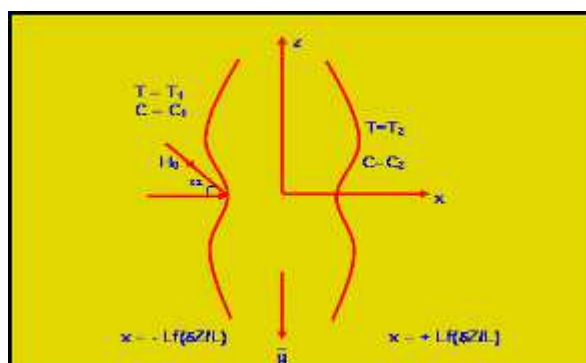
analyzed that the Flow and heat/mass transfer in a wavy duct with various corrugation angles in two dimensional flow regimes. Comini et al [5] have analyzed the Convective heat and mass transfer in wavy finned-tube exchangers.

In many chemical engineering processes, there does occur the chemical reaction between a foreign mass and the fluid in which the plate is moving. These processes take place in numerous industrial applications viz., polymer production, manufacturing of ceramics or glassware and food processing Das et al[6] have studied the effects of mass transfer on flow past an impulsively started infinite vertical plate with constant heat flux and chemical reaction. Muthukumara-swamy [22] has studied the effects of reaction on a long surface with suction. Recently Gnanaswar[9] has studied radiation and mass transfer on an unsteady two-dimensional laminar convective boundary layer flow of a viscous incompressible chemically reacting fluid along a semi-infinite vertical plate with suction by taking into account the effects of viscous dissipation.

The present trend in the field of chemical reaction analysis is to give a mathematical model for the system to predict the reactor performance. A large amount of research work has been reported in this field. In particular the study of heat and mass transfer with chemical reaction is of considerable importance in chemical and hydrometallurgical industries. Chemical reaction can be codified as either heterogeneous or homogeneous processes. This depends on whether they occur at an interface or as a single phase volume reaction. Frequently the transformations proceed in a moving fluid, a situation encountered in a number of technological fields. A common area of interest in the field of aerodynamics is the analysis of thermal boundary layer problems for two dimensional steady and incompressible laminar flow passing a wedge. Simultaneous heat and mass transfer from different geometrics embedded in a porous media has many engineering and geophysical application such as geothermal reservoirs, drying of porous solids thermal insulation, enhanced oil recovery, packed-bed catalytic reactors, cooling of nuclear reactors, and underground energy transport. A very significant area of research in radioactive heat transfer, at the present time is the numerical simulation of combined radiation and convection/conduction transport processes. The effort has arisen largely due to the need to optimize industrial system such as furnaces, ovens and boilers and the interest in our environment and in no conventional energy sources, such as the use of salt-gradient solar ponds for energy collection and storage. In particular, natural convection induced by the simultaneous action of buoyancy forces resulting from thermal and mass diffusion is of considerable interest in nature and in many industrial application such as geophysics, oceanography, drying process, solidification of binary alloy and chemical engineering. Kandaswamy et al[13] have discussed the Effects of chemical reaction, heat and mass transfer on boundary layer flow over a porous wedge with heat radiation in the presence of suction or injection

Recently, Jayasudha et al [12] has discussed the effect of magnetic field on unsteady convective heat and mass transfer flow in a vertical wavy channel with oscillatory flux with radiation absorption

In this paper we discuss the effect of chemical reaction, radiation and radiation absorption on unsteady free convective heat and mass transfer flow in a vertical wavy channel. The unsteadiness in the flow is due to the oscillatory flux in the flow region. The coupled equations governing the flow, heat and mass transfer have been solved by using a perturbation technique with the slope δ as the perturbation parameter. The expression for the velocity, the temperature, the concentration, the shear stress and the rate of heat and mass transfer are derived and are analyzed for different variations of the governing parameters G , R , M , β , N , N_1 , α , γ , k and t .



Formulation of the problem:

We consider the combined influence of radiation and chemical reaction on the unsteady motion of viscous, incompressible fluid in a vertical channel bounded by wavy walls. The thermal buoyancy in the flow field is created by an oscillatory flux in the fluid region. The walls are maintained at constant temperature and concentration. The Boussinesq approximation is used so that the density variation will be considered only in the buoyancy force. The

viscous and Darcy dissipations are neglected in comparison with heat by conduction and convection in the energy equation. Also the Kinematic viscosity ν , the thermal conducting k are treated as constants. We choose a rectangular Cartesian system $O(x, y)$ with x -axis in the vertical direction and y -axis normal to the walls. The walls of the channel are at $y = \pm L_f \left(\frac{\delta x}{L}\right)$

The equations governing the unsteady flow, heat and mass transfer are

Equation of continuity

$$\frac{\partial u}{\partial x} + \frac{\partial v}{\partial y} = 0 \quad (1)$$

Equation of linear momentum

$$\rho_e \left(\frac{\partial u}{\partial t} + u \frac{\partial u}{\partial x} + v \frac{\partial u}{\partial y} \right) = -\frac{\partial p}{\partial x} + \mu \left(\frac{\partial^2 u}{\partial x^2} + \frac{\partial^2 u}{\partial y^2} \right) - \rho g - (\sigma \mu_e^2 H_o^2) u \quad (2)$$

$$\rho_e \left(\frac{\partial v}{\partial t} + u \frac{\partial v}{\partial x} + v \frac{\partial v}{\partial y} \right) = -\frac{\partial p}{\partial y} + \mu \left(\frac{\partial^2 v}{\partial x^2} + \frac{\partial^2 v}{\partial y^2} \right) \quad (3)$$

Equation of Energy:

$$\rho_e C_p \left(\frac{\partial T}{\partial t} + u \frac{\partial T}{\partial x} + v \frac{\partial T}{\partial y} \right) = \lambda \left(\frac{\partial^2 T}{\partial x^2} + \frac{\partial^2 T}{\partial y^2} \right) - Q(T - T_e) + Q_1(C - C_e) - \frac{\partial(q_R)}{\partial y} \quad (4)$$

Equation of diffusion

$$\left(\frac{\partial C}{\partial t} + u \frac{\partial C}{\partial x} + v \frac{\partial C}{\partial y} \right) = D_1 \left(\frac{\partial^2 C}{\partial x^2} + \frac{\partial^2 C}{\partial y^2} \right) - k_1(C - C_e) \quad (5)$$

Equation of state

$$\rho - \rho_e = -\beta \rho_e (T - T_e) - \beta^* \rho_e (C - C_e) \quad (6)$$

where ρ_e is the density of the fluid in the equilibrium state, T_e, C_e are the temperature and concentration in the equilibrium state, (u, v) are the velocity components along $O(x, y)$ directions, p is the pressure, T, C are the temperature and Concentration in the flow region, ρ is the density of the fluid, μ is the constant coefficient of viscosity, C_p is the specific heat at constant pressure, λ is the coefficient of thermal conductivity, β is the coefficient of thermal expansion, Q is the strength of the constant internal heat source, σ is the electrical conductivity, μ_e is the magnetic permeability, β^* is the volumetric expansion with mass fraction coefficient D_1 , is the molecular diffusivity and k_1 is the chemical reaction coefficient.

$$\text{In the equilibrium state } 0 = -\frac{\partial p_e}{\partial x} - \rho_e g \quad (7)$$

where $p = p_e + p_D$, p_D being the hydrodynamic pressure.

The flow is maintained by an oscillatory volume flux for which a characteristic velocity is defined as

$$q(1 + k e^{i\omega t}) = \frac{1}{L} \int_{-L_f}^{L_f} u dy. \quad (8)$$

The boundary conditions for the velocity and temperature fields are

$$u = 0, v = 0, T = T_1, C = C_1 \quad \text{on } y = -Lf \left(\frac{\delta x}{L} \right)$$

$$u = 0, v = 0, T = T_2, C = C_2 \quad \text{on } y = +Lf \left(\frac{\delta x}{L} \right) \quad (9)$$

In view of the continuity equation we define the stream function ψ as

$$u = -\psi_y, v = \psi_x \quad (10)$$

Eliminating pressure p from equations (2) & (3) and using the equations governing the flow in terms of ψ are

$$[(\nabla^2 \psi)_t + \psi_x (\nabla^2 \psi)_y - \psi_y (\nabla^2 \psi)_x] = \nu \nabla^4 \psi - \beta g (T - T_0)_y - \beta^* g (C - C_0)_y - (\sigma \mu_e^2 H_o^2) \frac{\partial^2 \psi}{\partial y^2} \quad (11)$$

$$\rho_e C_p \left(\frac{\partial T}{\partial t} + \frac{\partial \psi}{\partial y} \frac{\partial T}{\partial x} - \frac{\partial \psi}{\partial x} \frac{\partial T}{\partial y} \right) = \lambda \nabla^2 T - Q(T - T_0) + Q_1 (C - C_0) + \frac{16 \sigma \cdot T_e^3}{\beta_R} \frac{\partial^2 T}{\partial y^2} \quad (12)$$

$$\left(\frac{\partial C}{\partial t} + \frac{\partial \psi}{\partial y} \frac{\partial C}{\partial x} - \frac{\partial \psi}{\partial x} \frac{\partial C}{\partial y} \right) = D \nabla^2 C - k_1 (C - C_0) \quad (13)$$

Introducing the non-dimensional variables in (9) & (10) as

$$x' = x/L, y' = y/L, t' = t\omega, \Psi' = \Psi/\nu, \theta = \frac{T - T_2}{T_1 - T_2}, C' = \frac{C - C_2}{C_1 - C_2} \quad (14)$$

the governing equations in the non-dimensional form (after dropping the dashes) are

$$R(\gamma^2 (\nabla^2 \psi)_t + \frac{\partial(\psi, \nabla^2 \psi)}{\partial(x, y)}) = \nabla^4 \psi + \left(\frac{G}{R} \right) (\theta_y + N C_y) - M^2 \frac{\partial^2 \psi}{\partial y^2} \quad (15)$$

$$P(\gamma^2 \frac{\partial \theta}{\partial t} + \frac{\partial \psi}{\partial y} \frac{\partial \theta}{\partial x} - \frac{\partial \psi}{\partial x} \frac{\partial \theta}{\partial y}) = \nabla^2 \theta - \alpha \theta + Q_1 C + \frac{4}{3N_1} \frac{\partial^2 \theta}{\partial y^2} \quad (16)$$

$$Sc(\gamma^2 \frac{\partial C}{\partial t} + \frac{\partial \psi}{\partial y} \frac{\partial C}{\partial x} - \frac{\partial \psi}{\partial x} \frac{\partial C}{\partial y}) = \nabla^2 C - KC \quad (17)$$

where

$$R = \frac{UL}{\nu} \quad (\text{Reynolds number}) \quad G = \frac{\beta g \Delta T_e L^3}{\nu^2} \quad (\text{Grashof number})$$

$$P = \frac{\mu c_p}{k_1} \quad (\text{Prandtl number}), \quad M^2 = \frac{\sigma \mu_e^2 H_o^2 L^2}{\nu^2} \quad (\text{Hartman Number}), \quad Sc = \frac{\nu}{D_1} \quad (\text{Schmidt Number})$$

$$\alpha = \frac{QL^2}{\lambda} \quad (\text{Heat source parameter}) \quad K = \frac{K_1 L^2}{D_1} \quad (\text{Chemical reaction parameter})$$

$$\gamma^2 = \frac{\omega L^2}{\nu} \quad (\text{Womersley number}) \quad Q_1 = \frac{Q_1 (C - C_e) L^2}{D_1 C_p} \quad (\text{Radiation absorption parameter})$$

$$\nabla^2 = \frac{\partial^2}{\partial x^2} + \frac{\partial^2}{\partial y^2}$$

The corresponding boundary conditions are

$$\psi(+f) - \psi(-f) = 1$$

$$\frac{\partial \psi}{\partial x} = 0, \quad \frac{\partial \psi}{\partial y} = 0 \quad \text{at } y = \pm f \quad (18)$$

$$\theta(x, y) = 1, C = 1 \quad \text{on } y = -f, \theta(x, y) = 0, C = 0 \quad \text{on } y = f, \frac{\partial \theta}{\partial y} = 0, \frac{\partial C}{\partial y} = 0 \quad \text{at } y = 0 \quad (19)$$

The value of ψ on the boundary assumes the constant volumetric flow in consistent with the hypothesis (7). Also the wall temperature varies in the axial direction in accordance with the prescribed arbitrary function t .

Method of Solution

The main aim of the analysis is to discuss the perturbations created over a combined free and forced convection flow due to traveling thermal wave imposed on the boundaries. The perturbation analysis is carried out by assuming that the aspect ratio δ to be small.

Introduce the transformation such that

$$\bar{x} = \delta x, \quad \frac{\partial}{\partial x} = \delta \frac{\partial}{\partial \bar{x}}$$

Then

$$\frac{\partial}{\partial x} \approx O(\delta) \rightarrow \frac{\partial}{\partial \bar{x}} \approx O(1)$$

For small values of $\delta \ll 1$, the flow develops slowly with axial gradient of order δ

$$\text{And hence we take } \frac{\partial}{\partial \bar{x}} \approx O(1)$$

Using the above transformation the equations (15-17) reduces to

$$\delta R (\gamma^2 (\nabla_1^2 \psi)_t + \frac{\partial(\psi, \nabla_1^2 \psi)}{\partial(x, y)}) = \nabla_1^4 \psi + \left(\frac{G}{R}\right)(\theta_y + NC_y) - M^2 \frac{\partial^2 \psi}{\partial y^2} \quad (20)$$

$$\delta P (\gamma^2 \frac{\partial \theta}{\partial t} + \frac{\partial \psi}{\partial y} \frac{\partial \theta}{\partial x} - \frac{\partial \psi}{\partial x} \frac{\partial \theta}{\partial y}) = \nabla_1^2 \theta - \alpha \theta + Q_1 C \quad (21)$$

$$\delta S_c (\gamma^2 \frac{\partial C}{\partial t} + \frac{\partial \psi}{\partial y} \frac{\partial C}{\partial x} - \frac{\partial \psi}{\partial x} \frac{\partial C}{\partial y}) = \nabla_1^2 C - KC \quad (22)$$

Where

$$\nabla_1^2 = \delta^2 \frac{\partial^2}{\partial x^2} + \frac{\partial^2}{\partial y^2}$$

Introducing the transformation

$$\eta = \frac{y}{f(\bar{x})}$$

the equations(3.1-3.3) reduces to

$$\delta R f (\gamma^2 (F^2 \psi)_t + \frac{\partial(\psi, F^2 \psi)}{\partial(\bar{x}, \eta)}) = F^4 \psi + \left(\frac{Gf^3}{R}\right)(\theta_\eta + NC_\eta) - (M^2 f^2) \frac{\partial^2 \psi}{\partial \eta^2} \quad (23)$$

$$\delta P (\gamma^2 \frac{\partial \theta}{\partial t} + f (\frac{\partial \psi}{\partial \eta} \frac{\partial \theta}{\partial x} - \frac{\partial \psi}{\partial x} \frac{\partial \theta}{\partial \eta})) = F^2 \theta - \alpha f^2 \theta + Q_1 f^2 C \quad (24)$$

$$\delta Sc(\gamma^2 \frac{\partial C}{\partial t} + f(\frac{\partial \psi}{\partial \eta} \frac{\partial C}{\partial x} - \frac{\partial \psi}{\partial x} \frac{\partial C}{\partial \eta})) = F^2 C - KC \tag{25}$$

Where

$$F^2 = \delta^2 \frac{\partial^2}{\partial \bar{x}^2} + \frac{\partial^2}{\partial \eta^2}$$

We adopt the perturbation scheme and write

$$\begin{aligned} \psi(x, \eta, t) &= \psi_0(x, \eta, t) + ke^{it} \bar{\psi}_0(x, \eta, t) + \delta(\psi_1(x, \eta, t) + ke^{it} \bar{\psi}_1(x, \eta, t)) + \dots \\ \theta(x, \eta, t) &= \theta_0(x, \eta, t) + ke^{it} \bar{\theta}_0(x, \eta, t) + \delta(\theta_1(x, \eta, t) + ke^{it} \bar{\theta}_1(x, \eta, t)) + \dots \\ C(x, \eta, t) &= C_0(x, \eta, t) + ke^{it} \bar{C}_0(x, \eta, t) + \delta(C_1(x, \eta, t) + ke^{it} \bar{C}_1(x, \eta, t)) + \dots \end{aligned} \tag{26}$$

On substituting (20) in (23) - (25) and separating the like powers of δ the equations and respective conditions to the zeroth order are

$$\psi_{0,\eta\eta\eta\eta} - (M_1^2 f^2) \psi_{0,\eta\eta} = -(\frac{Gf^3}{R})(\theta_{0,\eta} + NC_{0,\eta}) \tag{27}$$

$$\theta_{0,\eta\eta} - (\alpha f^2) \theta_0 = 0 \tag{28}$$

$$C_{0,\eta\eta} - (KScf^2) C_0 = 0 \tag{29}$$

With $\psi_{0(+1)} - \psi_{0(-1)} = 1$,

$$\psi_{0,\eta} = 0, \psi_{0,x} = 0 \quad \text{at } \eta = \pm 1 \tag{30}$$

$$\theta_o = 1, \quad C_o = 1 \quad \text{on } \eta = -1 \tag{31}$$

$$\theta_o = 0, \quad C_o = 0 \quad \text{on } \eta = 1$$

$$\bar{\theta}_{0,\mu\eta} - (iP\gamma^2 f^2) \bar{\theta}_0 = 0 \tag{32}$$

$$\bar{C}_{0,\eta\eta} - (KSc\gamma^2 f^2) \bar{C}_o = 0 \tag{33}$$

$$\bar{\psi}_{0,\eta\eta\eta\eta} - ((M_1^2 + i\gamma^2) f^2) \bar{\psi}_{0,\eta\eta} = -(\frac{Gf^3}{R})(\bar{\theta}_{0,\eta} + N\bar{C}_{0,\eta}) \tag{34}$$

$$\bar{\theta}_o(\pm 1) = 0 \quad \bar{C}_o(\pm 1) = 0$$

$$\bar{\psi}_o(+1) - \bar{\psi}_o(-1) = 1 \quad \bar{\psi}_{o,\eta}(\pm 1) = 0, \bar{\psi}_{o,x}(\pm 1) = 0 \tag{35}$$

The first order equations are

$$\psi_{1,\eta\eta\eta\eta} - (M_1^2 f^2) \psi_{1,\eta\eta} = -(\frac{Gf^3}{R})(\theta_{1,\eta} + NC_{1,\eta}) + (Rf)(\psi_{0,\eta} \psi_{0,x\eta\eta} - \psi_{0,x} \psi_{0,\eta\eta\eta}) \tag{36}$$

$$\theta_{1,\eta\eta} - (\alpha f^2) \theta_1 = (PRf)(\psi_{0,x} \theta_{o,\eta} - \psi_{0,\eta} \theta_{ox}) \tag{37}$$

$$C_{1,\eta\eta} - (KScf^2) C_1 = (Scf)(\psi_{0,x} C_{o,\eta} - \psi_{0,\eta} C_{ox}) \tag{38}$$

$$\begin{aligned} \bar{\psi}_{1,\eta\eta\eta\eta} - (M_1^2 + i\gamma^2) f^2 \bar{\psi}_{1,\eta\eta} &= -(\frac{Gf^3}{R})(\bar{\theta}_{1,\eta} + N\bar{C}_{1,\eta}) + (Rf)(\bar{\psi}_{0,\eta} \psi_{0,x\eta\eta} + \\ &+ \psi_{0,\eta} \bar{\psi}_{0,x\eta\eta} - \psi_{0,x} \bar{\psi}_{0,\eta\eta\eta} - \bar{\psi}_{0,x} \bar{\psi}_{0,\eta\eta\eta}) \end{aligned} \tag{39}$$

$$\bar{\theta}_{1,\eta\eta} - ((iP\gamma^2 + \alpha)f^2)\bar{\theta}_1 = (PRf)(\psi_{0,\eta}\bar{\theta}_{o,x} + \bar{\psi}_{0,\eta}\theta_{ox} - \bar{\psi}_{0,x}\theta_{o,\eta} - \psi_{0,x}\bar{\theta}_{o\eta}) \tag{40}$$

$$\bar{C}_{1,\eta\eta} - ((K + i\gamma^2)Scf^2)\bar{C}_1 = (Scf)(\psi_{0,\eta}\bar{C}_{o,x} + \bar{\psi}_{0,\eta}C_{ox} - \bar{\psi}_{0,x}C_{o,\eta} - \psi_{0,x}\bar{C}_{o\eta}) \tag{41}$$

With $\psi_{1(+1)}.\psi_{1(-1)} = 0$

$$\psi_{1,\eta} = 0, \psi_{1,x} = 0 \text{ at } \eta = \pm 1 \tag{42}$$

$$\theta_1(\pm 1) = 0 \quad C_1(\pm 1) = 0$$

$$\bar{\theta}_1(\pm 1) = 0 \quad \bar{C}_1(\pm 1) = 0$$

$$\bar{\psi}_1(+1) - \bar{\psi}_1(-1) = 1 \quad \bar{\psi}_{1,\eta}(\pm 1) = 0, \bar{\psi}_{1,x}(\pm 1) = 0$$

NUSSELT NUMBER and SHERWOOD NUMBER

$$(\tau)_{y=-1} = d_6 + Ecd_7 + \delta d_8 + O(\delta^2)$$

The local rate of heat transfer coefficient (Nusselt number Nu) on the walls has been calculated using the formula

$$Nu = \frac{1}{\theta_m - \theta_w} \left(\frac{\partial \theta}{\partial y} \right)_{\eta=\pm 1}$$

where

$$\theta_m = 0.5 \int_{-1}^1 \theta d\eta$$

and the corresponding expressions are

$$(Nu)_{\eta=+1} = \frac{(d_9 + \delta d_{11})}{(\theta_m - \text{Sin}(x + \gamma))}$$

$$(Nu)_{\eta=-1} = \frac{(d_8 + \delta d_{10})}{(\theta_m - 1)}$$

Where $\theta_m = d_{14} + \delta d_{15}$

The local rate of mass transfer coefficient (Sherwood Number Sh) on the walls has been calculated using the formula

$$Sh = \frac{1}{C_m - C_w} \left(\frac{\partial C}{\partial y} \right)_{y=\pm 1}$$

where $C_m = 0.5 \int_{-1}^1 C dy$

and the corresponding expressions are

$$(Sh)_{\eta=+1} = \frac{(d_4 + \delta d_6)}{(C_m)}, \quad (Sh)_{\eta=-1} = \frac{(d_5 + \delta d_7)}{(C_m - 1)}$$

Where $C_m = d_{12} + \delta d_{13}$ d_1, d_2, \dots, d_{14} are constants given in the appendix.

RESULTS AND DISCUSSION

In this analysis, we investigate the effect of chemical reaction, radiation and radiation absorption on unsteady convective heat and mass transfer flow of a viscous electrically conducting fluid in a vertical wavy channel

in the presence of heat generating sources. The axial velocity is shown in figure 1 – 5 for different values of α , Q_1 , β , N_1 , K .

An increase in the strength of the heat source reduces $|u|$ in fluid region. Also for every α , u exhibits a reversal flow in the entire flow region (fig.1). An increase in the radiation absorption parameter Q_1 results in an enhancement in $|u|$ in the lower half and reduces in the upper half of the channel (fig.2). The variation of u with radiation parameter N_1 shows that higher the radioactive heat flux ($N_1 \leq 1.5$) larger the axial velocity and for further higher values of $N_1 \geq 3.5$, we notice a depreciation in u (fig.2). The influence of the surface geometry on u is shown in fig.3. It is found that higher the constriction of the channel walls, larger $|u|$ for $\beta \leq 0.3$ and smaller for $\beta \geq 0.5$

The variation of u with chemical reaction parameter k shows that the axial velocity enhances with increase in k (fig.4).

The secondary velocity (v) which is due to the wall waviness of the channel is shown in figs 6-10

The variation of v with heat source parameter α shows that the magnitude of v enhances remarkably with increase in α in the lower half of the channel and depreciates in the upper half of the channel (fig.6). An increase in Q_1 leads to an enhancement in $|v|$ (fig.7). The variation of v with radiation parameter N_1 shows that higher the radioactive heat flux larger the secondary velocity (fig.8). From fig.9 we find that higher the constriction of the channel walls larger $|v|$ in the flow region. The variation of v with chemical reaction parameter k shows that $|v|$ enhances with increase in $k \leq 0.5$ and depreciates with higher $k \geq 1.5$ (fig.10).

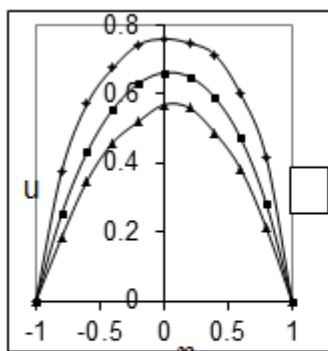


Fig.1 Variation of u with α

	I	II	III
α	2	4	6

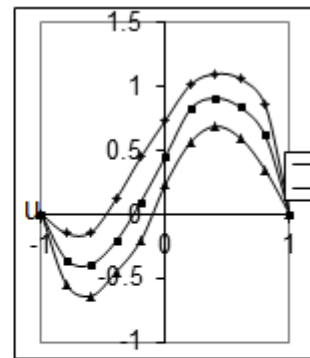


Fig.2 Variation of u with Q_1

	I	II	III
Q_1	2	4	6

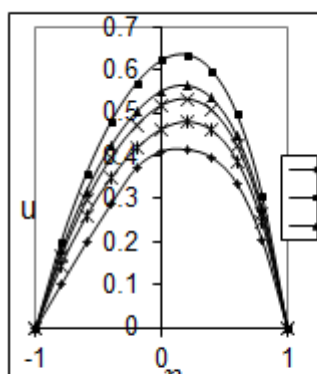


Fig.3 Variation of u with N_1

	I	II	III	IV	V
N_1	0.5	1.5	3.5	5	10

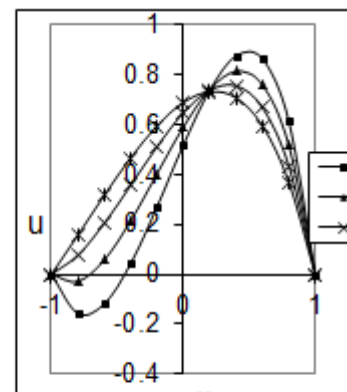


Fig.4 Variation of u with β

	I	II	III	IV	V
β	-0.1	-0.3	-0.5	-0.7	-0.9

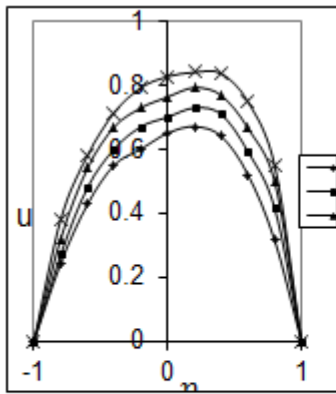


Fig.5 Variation of u with K
I II III IV
k 0.3 0.5 1.5 2.5

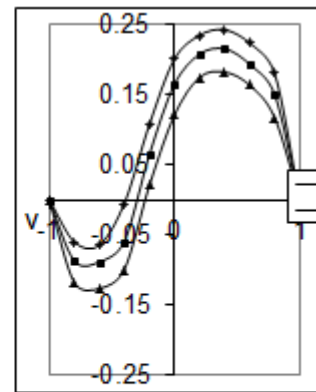


Fig.6 Variation of v with α
I II III
 α 2 4 6

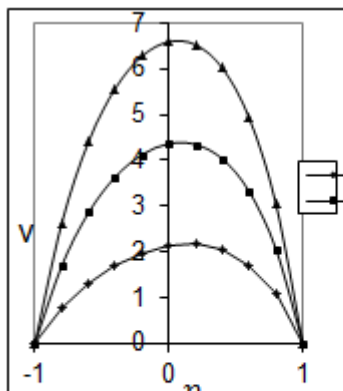


Fig.7 Variation of v with Q1
I II III
Q1 2 4 6

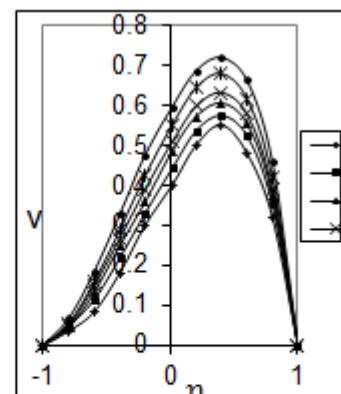


Fig.8 Variation of v with N1
I II III IV V
N1 0.5 1.5 3.5 5 10

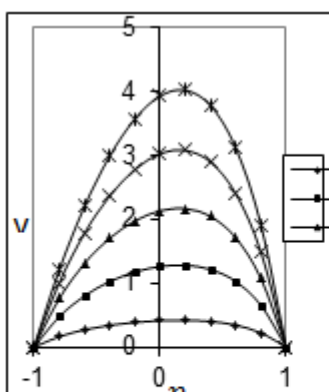


Fig.9 Variation of v with β
I II III IV V
 β -0.1 -0.3 -0.5 -0.7 -0.9

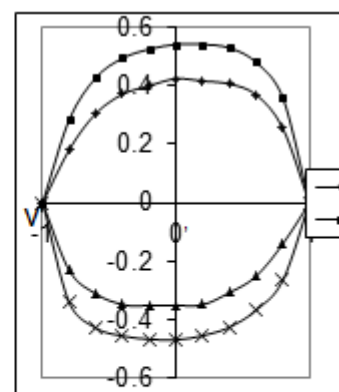


Fig.10 Variation of v with k
I II III IV
k 0.3 0.5 1.5 2.5

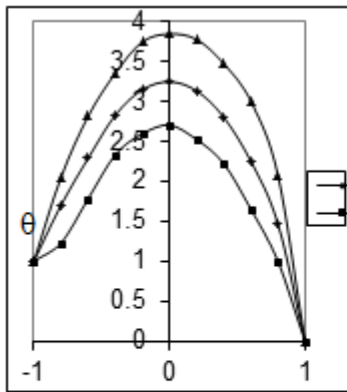


Fig.11 Variation of θ with α

	I	II	III
α	2	4	6

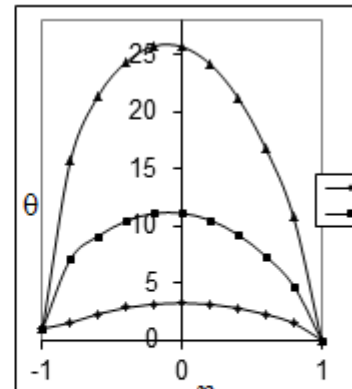


Fig.12 Variation of θ with $Q1$

	I	II	III
$Q1$	2	4	6

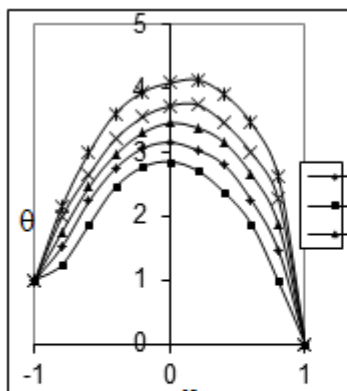


Fig.13 Variation of θ with $N1$

	I	II	III	IV	V
$N1$	0.5	1.5	3.5	5	1

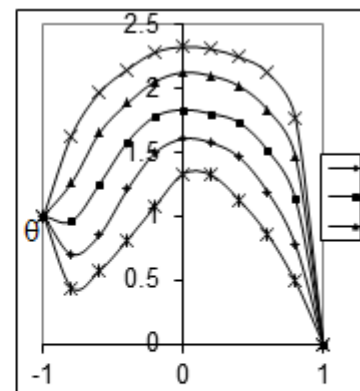


Fig.14 Variation of θ with β

	I	II	III	IV	V
β	-0.1	-0.3	-0.5	-0.7	-0.9

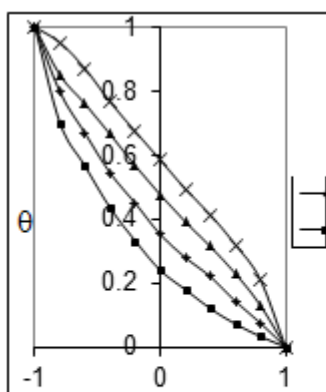


Fig.15 Variation of θ with k

	I	II	III	IV
k	0.3	0.5	1.5	2.5

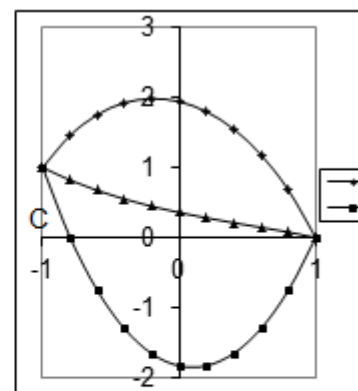


Fig.16 Variation of C with α

	I	II	III
α	2	4	6

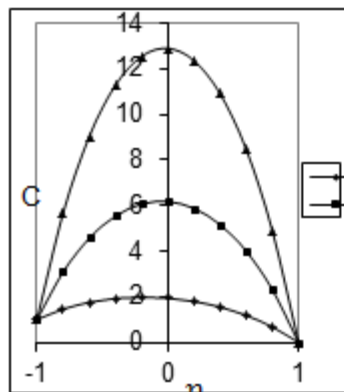


Fig.17 Variation of C with Q1

	I	II	III
Q1	2	4	6

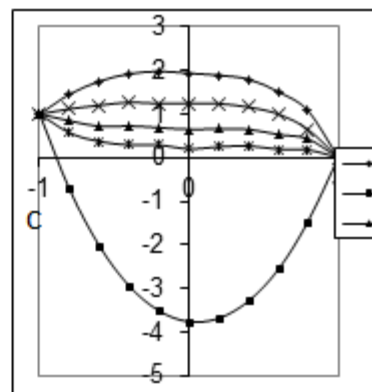


Fig.18 Variation of C with N1

	I	II	III	IV	V
N1	0.5	1.5	3.5	5	10

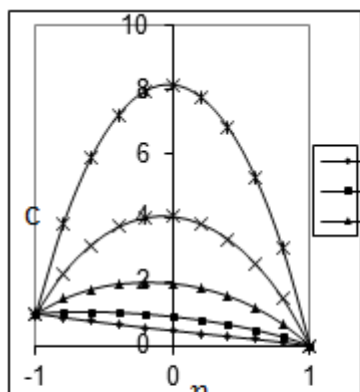


Fig.19 Variation of C with β

	I	II	III	IV	V
β	-0.1	-0.3	-0.5	-0.7	-0.9

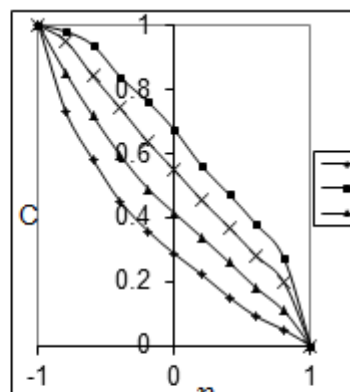


Fig.20 Variation of C with k

	I	II	III	IV
k	0.3	0.5	1.5	2.5

The non-dimensional temperature (θ) is shown in figures 11-15 for different parametric values. We follow the convention that the non-dimensional temperature is positive or negative according as the actual temperature is greater or lesser than T_2 . The variation of θ with heat source parameter α exhibits an increasing tendency with α (fig.11) From fig.12. We notice that the actual temperature enhances with increase in the radiation absorption parameter Q_1 . The variation of θ with N_1 shows that the actual temperature reduces with increase in $N_1 \leq 1.5$ and for higher $N_1 \geq 3.5$ we notice an enhancement in the actual temperature (fig.13). The influence of the wall waviness is shown in (fig.14). It is found that higher the constriction of the channel walls ($|\beta| \leq 0.7$) larger the actual temperature and for further higher constriction ($|\beta| \geq 0.9$) smaller the actual temperature. An increase in the chemical reaction parameter $k \leq 0.5$ leads to a depreciation in the actual temperature and again enhances with higher $k \geq 0.7$ (fig.15).

The non-dimensional concentration (C) is shown in figs 16-20 for different parametric values. An increase in the heat source parameter α (≤ 4) reduces the actual concentration and for higher $\alpha \geq 6$, we find an enhancement in C (fig.16). An increase in Q_1 enhances the actual concentration in the entire flow region (fig.17). The variation of C with N_1 shows that the actual concentration reduces with increase in $N_1 \leq 1.5$ and enhances with N_1 in the range $3.5 \leq N_1 \leq 5$ and again reduces for still higher $N_1 = 10$ (fig.18). Higher the constriction of the channel walls larger the actual concentration in the flow region (fig.19). For $k \leq 0.5$, we find that the actual concentration enhances in the region and for higher $k \geq 0.7$, it depreciates in the regions and for further higher $k \geq 0.9$, it increases in the flow region (fig.20). The rate of heat transfer (Nu) at $\eta = \pm 1$ is shown in tables 1-4 for different values of $G, \alpha, \beta, N_1, k, Q_1$. It is found that the rate of heat transfer enhances at $\eta = +1$ and reduces at $\eta = -1$ with $G > 0$ and for $G < 0$, we notice an enhancement at both the walls. The variation of Nu with chemical reaction parameter k shows that $|Nu|$ enhances with k at $\eta = \pm 1$. An increase in Q_1 reduces it at $\eta = +1$ and enhances at $\eta = -1$. With respect to the radiation parameter N_1 we find that $|Nu|$ reduces at $\eta = \pm 1$. Moving along the axial direction the Nusselt number reduces at

$\eta=+1$ and enhances at $\eta= -1$ for all G. higher the constriction of the walls larger the magnitude of rate of heat transfer at both walls (tables 1-4). The rate of mass transfer (Sh) at $\eta\pm 1$ is shown in tables 5-8 for different parametric values. An increase in $G>0$ enhances |Sh at $\eta = \pm 1$ while it enhances at $\eta = +1$ and reduces at $\eta = -1$ for $G<0$. An increase in the radiation absorption parameter Q_1 enhances the rate of mass transfer at $\eta=\pm 1$ in the heating case and in the cooling case, it reduces at both the walls. An increase in $k\leq 1.5$ enhances |Sh| and depreciates with higher $k\geq 2.5$ in the heating case and cooling case a reversed effect is observed in the behavior of |Sh| at $\eta=+1$. At $\eta = -1$ the rate of mass transfer depreciate increase in k for all G. The variation of Sh with radiation parameter N_1 shows that higher the radioactive heat flux ($N_1\leq 3.5$) smaller Sh at $\eta=1$ and enhances at $\eta=-1$ while a reversed effect is noticed for higher $N_1\geq 5$ for all G. Higher the constriction of the channel walls larger |Sh| at $\eta = +1$ and smaller $\eta = -1$. (tables 5-8)

Table-1 Nu at $y= +1$ ($\beta<0$)

G	I	II	III	IV	V	VI	VII
10	-2.67594	-3.5283	1.30452	-1.7498	-3.3163	-4.68442	-8.2131
30	-1.81281	-3.5339	1.31318	-1.3925	-2.0329	-3.10006	-5.4756
50	-1.43725	-3.5435	1.32165	-1.1924	-1.5497	-2.37827	-4.1627
-10	-6.4516	-3.5264	1.29568	-2.5355	-15.154	-10.8727	-17.413
-30	8.88845	-3.5281	1.28665	-5.4921	4.45677	23.1316	94.8729
-50	2.28471	-3.5335	1.27742	14.235	1.72253	5.16662	12.1438
α	2	4	6	2	2	2	2
k	0.5	0.5	0.5	1.5	2.5	0.5	0.5
Q_1	2	2	2	2	2	4	6

Table-2 Nu at $y= +1$

G	I	II	III	IV	V	VI	VII	VIII	IX	X
10	-2.675	-2.883	-3.017	-1.9203	-1.1544	-2.421	0.66609	0.79491	-18.738	0.1747
30	-1.812	-2.854	-2.604	-1.0274	-0.5343	-2.427	0.57328	0.75359	52.2674	0.05614
50	-1.437	-2.832	-2.341	-0.7547	-0.3877	-2.438	0.47111	0.70725	12.7154	0.0357
-10	-6.451	-2.921	-3.745	25.4903	2.4456	-2.421	0.74736	0.83058	-7.0357	-0.1211
-30	8.8884	-2.971	-5.348	1.42868	0.54786	-2.425	0.81491	0.85993	-3.9769	-0.0417
-50	2.2847	-3.040	-11.60	0.6964	0.31515	-2.435	0.86661	0.88228	-2.5839	-0.0243
β	-0.5	-0.1	-0.3	-0.7	-0.9	-0.5	-0.5	-0.5	-0.5	-0.5
N_1	0.5	0.5	0.5	0.5	0.5	1.5	3.5	5	10	100

Table-3 Nu at $y= -1$

G	I	II	III	IV	V	VI	VII
10	-1.415	-3.2155	1.67056	-5.05784	-2.3205	-3.6507	-7.54666
30	-1.0119	-3.2171	1.67646	-0.16649	-1.4493	-2.3887	-4.91837
50	-0.8607	-3.2212	1.68221	-0.23301	-1.1394	-1.8408	-3.70814
-10	-3.5612	-3.2161	1.6645	0.17951	-14.351	-9.4774	-17.5644
-30	2.44292	-3.2188	1.65828	1.39272	2.26379	10.9998	42.11716
-50	0.62177	-3.2238	1.65188	-1.79244	0.84683	3.11893	9.10072
α	2	4	6	2	2	2	2
k	0.5	0.5	0.5	1.5	2.5	0.5	0.5
Q_1	2	2	2	2	2	4	6

Table-4 Nu at $y= -1$

G	I	II	III	IV	V	VI	VII	VIII	IX	X
10	-1.415	-1.4334	-1.559	-1.055	-0.6897	-2.462	2.76119	1.99666	1.32351	-0.1174
30	-1.011	-1.5470	-1.446	-0.6028	-0.3425	-2.468	2.51665	1.89821	1.36053	-0.0332
50	-0.860	-1.6416	-1.381	-0.4747	-0.2673	-2.482	2.26348	1.79622	1.39704	-0.0170
-10	-3.561	-1.2932	-1.786	7.74073	1.30385	-2.461	2.99105	2.09069	1.28514	0.10987
-30	2.4429	-1.1140	-2.411	0.60101	0.28887	-2.466	3.19939	2.17933	1.23295	0.04098
-50	0.6217	-0.8744	-9.217	0.27324	0.16835	-2.477	3.37805	2.26151	1.22479	0.02604
β	-0.5	-0.1	-0.3	-0.7	-0.9	-0.5	-0.5	-0.5	-0.5	-0.5
N_1	0.5	0.5	0.5	0.5	0.5	1.5	3.5	5	10	100

Table-5 Sh at $y=+1$

G	I	II	III	IV	V	VI	VII
10	7.38657	-1.6401	0.37588	10.4829	5.60425	5.19517	2.92027
30	5.96968	-1.608	0.45977	9.04038	4.47083	4.24619	2.55381
50	5.61502	-1.5751	0.5415	8.52888	4.29743	3.82286	2.35177
-10	13.04088	-1.6717	0.28973	14.2266	11.9016	7.69594	3.63662
-30	-10.6524	-1.7029	0.20117	-28.887	-16.037	21.3906	5.3555
-50	-8.38811	-1.7338	0.11008	-8.7979	-4.0945	-17.9229	-13.152
α	2	4	6	2	2	2	2
k	0.5	0.5	0.5	1.5	2.5	0.5	0.5
Q_1	2	2	2	2	2	4	6

Table-6 Sh at $y=+1$

G	I	II	III	IV	V	VI	VII	VIII	IX	X
10	7.3865	6.3641	6.6785	8.6091	10.53	-1.83	1.6920	1.8049	1.8194	1.7943
30	5.9696	6.2364	5.7534	6.7220	7.9421	-1.79	1.7801	1.9061	1.9579	1.9873
50	5.61502	6.13042	5.30861	6.69013	8.4119	-1.7437	1.85456	1.98536	2.06269	2.13101
-10	13.040	6.5208	8.7704	23.5	78.093	-1.87	1.5866	1.6756	1.6376	1.5380
-30	-10.652	6.71778	15.4762	-14.496	-9.0411	-1.9019	1.45821	1.50965	1.39994	1.20021
-50	-8.3881	6.97309	5.9254	-5.013	-4.1493	-1.9274	1.29896	1.29501	1.08888	0.75655
β	-0.5	-0.1	-0.3	-0.7	-0.9	-0.5	-0.5	-0.5	-0.5	-0.5
N_1	0.5	0.5	0.5	0.5	0.5	1.5	3.5	5	10	100

Table-7 Sh at $y=-1$

G	I	II	III	IV	V	VI	VII
10	99.4679	10.0852	-5.118	50.7541	27.4053	28.5623	14.37309
30	19.0754	10.0032	-5.314	55.3241	9.73522	12.9974	9.49697
50	10.7041	9.92547	-5.5175	65.0359	5.52738	8.3546	7.04533
-10	-24.73	10.1723	-4.9291	-22.0313	-27.674	-109.46	29.66949
-30	-9.2471	10.265	-4.7469	-12.5527	-7.4845	-17.043	-3.0234
-50	-4.7453	10.3644	-4.5711	-7.86091	-3.4094	-8.4965	-23.4733
α	2	4	6	2	2	2	2
k	0.5	0.5	0.5	1.5	2.5	0.5	0.5
Q_1	2	2	2	2	2	4	6

Table-8 Sh at $y=-1$

G	I	II	III	IV	V	VI	VII	VIII	IX	X
10	99.4679	-14.9	-47.544	33.8866	24.9648	8.56221	-9.875	-8.28	-7.78	-7.969
30	19.0754	-20.0	92.0205	12.4091	9.9698	8.50518	-12.36	-10.3	-9.93	-10.56
50	10.7041	-28.9	25.3154	7.09221	4.94143	8.46063	-16.33	-13.6	-13.4	-15.18
-10	-24.73	-11.6	-17.152	-33.109	-38.338	8.63524	-8.144	-6.84	-6.34	-6.315
-30	-9.2471	-9.28	-9.6197	-8.5016	-7.6234	8.73013	-6.856	-5.788	-5.31	-5.170
-50	-4.7453	-7.54	-6.1424	-3.5873	-2.6495	8.85675	-5.848	-4.968	-4.52	-4.3348
β	-0.5	-0.1	-0.3	-0.7	-0.9	-0.5	-0.5	-0.5	-0.5	-0.5
N_1	0.5	0.5	0.5	0.5	0.5	1.5	3.5	5	10	100

CONCLUSION

The axial velocity enhances with increase in the chemical reaction parameter k. The secondary velocity $|v|$ enhances with increase in $k \leq 0.5$ and depreciates with higher $k \geq 1.5$. An increase in $k \leq 0.5$ leads to depreciation in the actual temperature and again enhance with higher $k \geq 0.5$. For $k \leq 0.5$, we find that the actual concentration enhances in the region and for higher $k \geq 0.7$, it depreciates in the regions and for further higher $k \geq 0.9$, it increase in the flow region. an increase in $k \leq 1.5$, reduces $|Nu|$ at $\eta=+1$ and enhances at $\eta=-1$ and for higher $k \geq 2.5$, we notice an enhancement in $|Nu|$ at both the walls. The variation of Sh with chemical reaction parameter k shows that higher the chemical reaction parameter $k < 1.5$ smaller $|Sh|$ with increase in $k \leq 1.5$ and for higher $k \geq 2.5$.

An increase in Q_1 results in an enhancement in $|u|$ in the lower half and reduces in the upper half of the channel. An increase in Q_1 leads to an enhancement in $|v|$, θ and C. An increase in $Q_1|Nu|$ reduces at $\eta=+1$ and enhances at $\eta=-1$. An increase in Q_1 enhances the rate of mass transfer at $\eta=\pm 1$ in the heating case and in the cooling case, it reduces at both the walls.

Higher the radioactive heat flux ($N_1 \leq 1.5$) larger the axial velocity and depreciates for higher values of $N_1 \geq 3.5$. Higher the radioactive heat flux larger the secondary velocity. The actual temperature reduces with increase in $N_1 \leq 1.5$ and for higher $N_1 \geq 3.5$ an enhancement in the actual temperature. The actual concentration reduces with increase in $N_1 \leq 1.5$ and enhances with N_1 in the range $3.5 \leq N_1 \leq 5$ and again reduces for still higher $N_1 = 10$. $|Nu|$ reduces at $\eta = \pm 1$ with increase in $N_1 \leq 3.5$ and for higher $N_1 \geq 5$, a reversed effect is noticed in the behavior of $|Nu|$. The variation of Sh with radiation parameter N_1 shows that higher the radioactive heat flux ($N_1 \leq 3.5$) smaller Sh at $\eta = 1$ and enhances at $\eta = -1$ while a reversed effect is noticed for higher $N_1 \geq 5$.

The axial velocity u exhibits a reversal flow in the entire flow region for every value of α . the secondary velocity $|v|$ enhances with increase in α in the lower half of the channel and depreciates in the upper half of the channel. An increase in α results in an enhancement in θ . An increase in $\alpha (\leq 4)$ reduces the actual concentration and for higher $\alpha \geq 6$, an enhancement in C . $|Nu|$ enhances with increase in the strength of the heat generating source ($\alpha \leq 4$) and reduces Nu with higher $\alpha \geq 6$ at $\eta = \pm 1$ for all G . Sh reduces at $\eta = 1$ and enhances at $\eta = -1$ with increase in $\alpha \leq 4$ and for higher $\alpha \geq 6$, it reduces at $\eta = \pm 1$ for all G .

Larger $|u|$ for $\beta \leq 0.3$ and smaller for $|\beta| \geq 0.5$ in the lower half and in the upper half it reduces in the flow region. Higher the constriction of the channel walls larger $|v|$ in the flow region. Larger the actual temperature for ($|\beta| \leq 0.7$) and for ($|\beta| \geq 0.9$) smaller the actual temperature. The variation of Nu with β shows that higher the constriction of the channel walls ($|\beta| \leq 0.3$) larger the rate of heat transfer and for further higher constriction $|\beta| \geq 0.5$, Nu reduces at both the walls. Higher the constriction of the channel walls ($|\beta| \leq 0.3$), the rate of mass transfer reduces at $\eta = 1$ and enhances at $\eta = -1$. For further higher $|\beta| \geq 0.7$, it enhances at $\eta = 1$ and reduces at $\eta = -1$.

REFERENCES

- [1] Angirasaa, D., Peterson, G. P. and Pop, I.: *International Journal of Heat Mass Transfer*, **1997**, 40, 2755-2773.
- [2] Bejan, A. and Khair, K. R.: *International Journal of Heat Mass Transfer*, **1985**, 28, 908-918.
- [3] Chamkha, A. J., Takhar, H. S. and Soundalgekar, V. M., *Chem. Engg. J.*, **2003**, 84, 104.
- [4] Cheng, P., *Advanced Heat Transfer*, **1978**, 14, 1-105.
- [5] Comini, G., C. Nonino and S. Savino, *International journals of Numerical Methods for Heat and Fluid flow*, **2002**, 12, 735-755.
- [6] Das, U. N., Deka, R. K. and Soundalgekar, V. M.: *Forschung in Inge.*, **1994**, 80, 284.
- [7] Deshikachar, K. S. and Ramachandra Rao, A., *International Journal of Engg Sci*, **1985**, 23, 1121.
- [8] Gagan S., Proceedings of natural heat and mass transfer conference Visakhapatnam, India **1985**.
- [9] Gnaneswar reddy: *Acta Ciencia Indica*, **2008**, 34, 21, 639.
- [10] Hussain, M. A. and Takhar, H. S.: *Heat and Mass transfer*, **1996**, 31, 43.
- [11] Hyan Goo Kwon, Sang Dong Hwang, Hyung Hee Cho, *Heat and Mass Transfer* **2008**, 45, 157-165.
- [12] Jayasudha : Jayasudha. J. S., U. Rajeswara Rao, and DRV Prasada Rao. *International Journal of Mathematical Archive* **2015**, 6.3, 2229-5046.
- [13] Kandaswamy .P., Abd. Wahid B. Md. Raj, azme B. Khamis, *Theoret. Appl. Mech.* **2006**, 33.2, 123-148.
- [14] Lai, F. C., *International Commn. heat mass transfer*, **1971**, 18, 93-106.
- [15] Lai, F. C. and Kulacki, F. A.: *International Journal of Heat Mass Transfer*, **1991**, 34, 1189-1194.
- [16] Lee, T. S., Parikh, P. G., Archivos, A. and Bershader, D., *International Journal of Heat Mass Transfer* **1982**, 25, 499-522.
- [17] Mabunni, R., Rajeswara Rao, U. and Prasada Rao, D. R. V.: *International Journal of Emerend Trend. in Engg. Dev.*, **2014**, 4.4, 137-150.
- [18] Madhusadana Reddy. Y., Ph.D. thesis, S.K. University, (Anantapur, India **2010**).
- [19] McMichael, M. and Deutsch. S., *Physics of Fluids*, **1984**, **27.1**, 110-118.
- [20] Murthy, P. V. S. N. and Singh, P. *Acta Mech.*, **1990**, 26, 567.
- [21] Muthukumaraswamy. R. and Ganesan, P., *International Journal of Applied. Mech and Engng.* **2003**, 44, 104.
- [22] Muthukumaraswamy, R., *Acta Mechnica*, **2002**, 155, 65.
- [23] Nelson, D. J. and Wood, B. D., *Heat transfer*, **1986**, 4, 1587-1952.
- [24] Nelson, D. J. and Wood, B. D., *International Journal of Heat Mass transfer*, **1989**, 82, 1789-1792.
- [25] Prakash, J. and Ogulu: *International Journal of Pure and Applied Maths*, **2006**, 44, 805.
- [26] Prasad, V., Kulacku, F. A. and Keyhani, M., *Journal of Fluid Mech.* **1985**, 150, 89-119.
- [27] Prasada Rao, D. R. V., Krishna, D. V. and Debnath, L., *International journal of Engg. Sci.* **1983**, 21, 9, 1025-1039.
- [28] Raptis, A. and Takhar, H. S.: *Heat and Mass transfer*, **1996**, 31, 243.
- [29] Raptis, A. A. and Perdikis, C., *Applied Mechanical Eng*, **1999**, 4, 817-821.
- [30] Soundalgekar, V. M. and Takhar, H. S.: *Modeling measurement and control*, **1993**, 51, 31,
- [31] Sree Ramachandra Murthy, A. Ph.D thesis, S.K. University, (Anantapur, India. **1992**)
- [32] Sparrow, E. M., Chryser, M. and Azvedo, L. F. A.: *Journal of Heat transfer*, **1984**, 106, 325-332.

- [33] Sparrow, E.M and Azvedo, L.F.A : *Journal of Heat and Mass transfer*, **1985**, 28, 1847-1857.
- [34] Sudha Mathew: Ph.D thesis, S.K. University, (Anantapur, India **2009**).
- [35] Trevison, D.V and Bejan, A : *ASME*, **1987**, 109, 104-111.
- [36] Vajravelu K and Ali Neyfeh. *International Journal of Maths and Math. Sc.* **1981**, 4, 805-818.
- [37] Vajravelu, K and Sastry, K.S. *Journal of Fluid Mech.* **1978**, 86, 2, 365.
- [38] Vajravelu, K and Debnath, L : *Acta Mech.* 59, 233-249.
- [39] Wei-Mon Yan: *International journal of Heat Mass transfer*, **1996**, 39, 1479-1488.